Q Estimation via Continous Wavelet Transform

Hormoz Izadi, Kris Innanen and Michael P. Lamoureux

ABSTRACT

In seismic signal analysis, irregular structures and points of sharp variation contain critical information, thus making the study of a signal's local properties an appropriate mechanism for obtaining information from seismic data. The local regularity of a seismic event is determined by the wavelet transform modulus maxima and the associated Lipschitz exponent. As a means of classifying regularities of a signal and estimating the associated Lipschitz exponent, the linear and non-linear Mallat-Hwang-Zhong (MHZ) signal model based on the wavelet theory is reviewed and developed.

For practical settings, in particular band-limited signal events, the more complex non-linear MHZ signal model must minimised in order to estimate the local regularity and the additional smoothness parameter. Based on synthetic vertical seismic profile (VSP) modelling, a relatively complicated mathematical mapping between the Lipschitz exponent and seismic quality factor Q is obtained. However, analysing the smoothness parameter results in an invertible power law relation between the aforementioned parameter and Q.

Applying the non-linear MHZ model to Ross Lake VSP field data captures the general absorption trend estimated by Zhang and stewart (2006). Furthermore, the power law relation provides relatively reasonable Q values comparable to the estimated values using traditional methods, such as the steepest descent. However, for a more robust mathematical relation between the Lipschitz exponent, smoothness parameter and seismic quality factor Q, additional theoretical and field data analysis is required.

INTRODUCTION

Singularities and points of sharp variation carry critical information that are typically amongst the most important features for analysing properties of transient signals or images (Mallat and Zhong, 1992). Points of sharp variation created by shadows, occlusions, highlights are typically located at boundaries of image structures and contain different intensity profiles (Mallat and Zhong, 1992). In seismic signal analysis, regions of abrupt change classifiable as "edges", contain considerable amount of a signal's information, thus making edge detection a potentially appropriate and efficient tool for obtaining information from seismic data (Innanen, 2003). Edge detection requires analysis of local properties of corresponding edges.

Traditionally, the Fourier transform has been the main mathematical tool and technique for analysing singularities and irregular structures. However, a major drawback lies in the fact that the Fourier transform generally provides a description of a signal's overall singularity, thus it is not well suited for finding spatial distributions and locations of singularities (Mallat and Zhong, 1992; Mallat and Hwang, 1992).

Applying advanced mathematical techniques namely continuous wavelet transform enables us to obtain the modulus maxima from seismic data and estimate the Lipschitz expo-

nents which in turn allows us to measure the local regularity of functions and differentiate the intensity profile of different edges (Mallat and Zhong, 1992; Mallat and Hwang, 1992).

Several important physical processes can in principle affect the local regularity of a reflected event in a seismic trace: processes of absorption/wave attenuation, and reflections from targets composed of thin (sub-wavelength) layers. It is generally understood that due to absorption, the energy of seismic waves propagating through an anelastic medium would dissipate over a given distance. As a result, transient waveforms are distorted as they propagate through such media; progressive loss of amplitudes and changes of phase are typically encountered (Kjartansson, 1979; Zhang, 2008). The overall effect of seismic attenuation is described by the dimensionless quality factor Q, with studies in seismic data processing concentrating on modelling, estimation or compensation (Innanen, 2003). In practical terms, estimation and compensation can potentially enhance the resolving power of seismic data. A robust estimation of Lipschitz exponents from seismic data, alongside prior geological information, could potentially lead to processing and inversion algorithms able to discern and characterise such targets. Algorithms of this kind would be of significant scientific and economic value.

SEISMIC SIGNAL SMOOTHNESS & LIPSCHITZ REGULARITY

Compared to the existing time-frequency transformations, the continuous wavelet transform provides a mathematical description of a function's local behaviour. The local regularity or behaviour of a seismic event is determined by the wavelet transform modulus maxima and the associated Lipschitz exponent. As a means of classifying regularities of a seismic signal and estimating the associated Lipschitz exponent, a linear and non-linear Mallat-Hwang-Zhong (MHZ) signal model based on the wavelet theory is reviewed.

For certain kind of signal events (impulse type events), a the linear model can be applied in order to determine the associated Lipschitz regularity. However, for band-limited signal events with some degree of smoothness a more complex non-linear model has to be applied. The non-linear signal model includes three parameters (as opposed to two for the linear model), in order to fully reflect and characterise a propagating seismic pulse as it experiences smoothness and loss of amplitude due to absorption. Hence, in order to estimate the associated parameters (mainly the local regularity and smoothness), one would need to apply the least squares method or a non-linear optimisation method such as the steepest descent.

Continuous wavelet transform

The wavelet transform divides a given function or signal into different scale components, and assigns a frequency range to each scale component by utilising a scalable modulated window, that calculates the spectrum at every position and shifts the scalable window along the signal, hence providing a time-scale representation of a given function or signal (Qian, 2002). In the short-time Fourier transform, the size of the windowed function is fixed regardless of the number of oscillations, whereas a wavelet adjusts the width, essentially keeping the number of oscillations constant (Qian, 2002).

Mathematically, for a given function $f(t)$ the continuous wavelet transform is given by the following relation,

$$\mathbf{W}f(s,\tau) = \frac{1}{\sqrt{s}} \int_{-\infty}^{+\infty} f(t)\psi^*(\frac{t-\tau}{s})dt, \tag{1}$$

where s represents the scaling factor inversely proportional to the frequency, τ represents translation along the time axis and $\psi^*(.)$ denotes the complex conjugate of the *"mother wavelet"* $\psi(t)$ (Gao and Yan, 2011; Qian, 2002). Mathematically, dilation (scaling) and translation (time-shifting) of the mother wavelet produces a family of wavelets.

Based on the continuous wavelet transform, a function $f(x)$ is said to be uniformly Lipschitz α over $[a,b]$ if and only if there exists a constant $A > 0$ such that the wavelet transform satisfies the following (Mallat and Zhong, 1992; Innanen, 2003),

$$|\mathbf{W}_s f(x)| < As^{\alpha} \tag{2}$$

where $|\mathbf{W}f(x)|$ is the modulus maxima of the function $f(x)$ at various scales $s = 2^j$ for $j\varepsilon\mathbb{Z}$. Equation 2 suggests that the evolution of the modulus of the wavelet coefficients across the scale depends on the local Lipschitz regularity of the desired function (Innanen, 2003). Thus, based on the properties associated with the Lipschitz exponent, a distinction could be made between singular and differentiable function (Mallat and Zhong, 1992; Hermann, 1997)

Estimating Lipschitz regularity

In order to estimate the Lipschitz exponent α from the data, one could linearise equation 2 by taking the logarithms in order to obtain the following relation,

$$\log_2 |\mathbf{W}_s f(x)| \leq \log_2 |A| + \alpha \log_2(s). \tag{3}$$

For $s = 2^j$, equation 3 reduces to the following expression,

$$\log_2 |\mathbf{W}_s f(x)| \leq \log_2 |A| + \alpha j. \tag{4}$$

Finding the slope and intercept of the relation given above (4), yields an estimate for α and A. Although linearising equation 2 simplifies the estimation of α, nevertheless this procedure requires certain degree of caution since it involves scaling the errors associated with the numerical estimation of the modulus maxima. Additionally one could estimate α and A by posing equation 4 as an optimisation problem. Forming the objective function, one would obtain the following expression

$$\phi(\alpha, A) = \sum_{i,j=1}^{n} [\log_2 |a_i| - (\log_2 |A| + \log_2(s_j))]^2, \tag{5}$$

where $a_i = \left|\mathbf{W}_{s_j} f(x)\right|$ and $s_j = 2^j$ for $i, j = 1, 2, 3, ..., n$. Minimising the objective function provides the following system of equations (Burden and Douglas, 2005)

$$\begin{pmatrix} A \\ \alpha \end{pmatrix} = \begin{pmatrix} n & \sum_{j=1}^{n} \log_2(s_j) \\ \sum_{j=1}^{n} \log_2(s_j) & \sum_{j=1}^{n} [\log_2(s_j)]^2 \end{pmatrix}^{-1} \begin{pmatrix} \sum_{i=1}^{n} \log_2(a_i) \\ \sum_{j=1}^{n} \log_2(s_j) . \sum_{i=1}^{n} \log_2(a_i) \end{pmatrix}. \quad (6)$$

The Mallat-Hwang-Zhong (MHZ) signal model

In seismic signal analysis, our main interest rests on estimating Lipschitz values ranging from $-1 \leq \alpha \leq 0$. Thus it is preferable to use a wavelet with a single vanishing moment, such as the first derivative of a Gaussian function. A wavelet $\psi(x)$ is said to have n vanishing moments if for $k < n$ it satisfies (Mallat and Hwang, 1992),

$$\int_{-\infty}^{+\infty} x^k \psi(x) dx = 0. \quad (7)$$

Furthermore, letting $\psi(x) = \frac{d\theta(x)}{dx}$, where $\theta(x)$ is a Gaussian function, and taking the continuous wavelet transform of f we obtain the following expression (Mallat and Hwang, 1992)

$$\mathbf{W}_s f(x) = f * (s\frac{d\theta_s}{dx})(x) = s\frac{d}{dx}(f * \theta_s)(x). \quad (8)$$

Based on equation 8, the local extrema of $\mathbf{W}_s f(x)$ corresponds to the inflection points of $f * \theta_s(x)$. Hence, the inflection points or points of sharp variation corresponding to $f * \theta_s(x)$ could be detected by estimating the local extrema of $|\mathbf{W}_s f(x)|$ (Mallat and Zhong, 1992).

Due to absorption and loss of energy, a pulse undergoes a degree of smoothness, thus gradually obtaining spectral characteristics of a Gaussian. To model and measure the smoothness of the signal variation, a delta function $h(x)$ is convolved with a Gaussian of variance σ^2 (Mallat and Zhong, 1992),

$$f(x) = h(x) * g_\sigma(x) \quad (9)$$

where $g_\sigma(x) = \frac{1}{\sqrt{2\pi}\sigma} \exp\left(\frac{-x^2}{2\sigma^2}\right)$. The continuous wavelet transform of 9 is given by the following

$$\mathbf{W}_s f(x) = 2^j \frac{d}{dx}(h * \theta_{s_0})(x) = \frac{2^j}{s_0} \mathbf{W}_{s_0} h(x) \quad (10)$$

where $\theta_{s_0} = g_\sigma(x) * \theta_s$ and $s_0 = \sqrt{2^{2j} + \sigma^2}$. As a result, the modulus maxima and Lipschitz regularity is given by the following relation (Mallat and Zhong, 1992; Mallat and Hwang, 1992),

$$|\mathbf{W}_{s_0} h(x)| = \frac{s_0}{s} |\mathbf{W}_{s_0} f(x)| \leq A s_0^\alpha \quad (11)$$

or

$$|\mathbf{W}_{s_0} f(x)| \leq s A s_0^{\alpha - 1}. \quad (12)$$

Taking the logarithm of 12 provides the following expression

$$\log_2 |a_i| \leq \log_2 |A| + j - \frac{\alpha - 1}{2} \log_2(\sigma^2 + 2^{2j}) \tag{13}$$

where $a_i = |\mathbf{W}_{s_0} f(x)|$. Minimising the objective function given by 12 requires the least squares method or a non-linear optimisation method such as the steepest descent.

Despite the fact that 4 trends towards non-linearity as σ increases, one could apply linear least squares method by reframing 4 as a linear model

$$y = a_0 + a_1 x \tag{14}$$

where $y = \log_2 |a_i| + j$, $a_0 = \log_2 |A|$ and $a_1 = \frac{\alpha - 1}{2}$. The solution to 14 is given by (Burden and Douglas, 2005)

$$a_0 = \frac{\sum_{i=1}^{n} x_i^2 \sum_{i=1}^{n} y_i - \sum_{i=1}^{n} x_i y_i \sum_{i=1}^{n} x_i}{n(\sum_{i=1}^{n} x_i^2) - (\sum_{i=1}^{n} x_i)^2} \tag{15}$$

and

$$a_1 = \frac{n\sum_{i=1}^{n} x_i y_i - \sum_{i=1}^{n} x_i \sum_{i=1}^{n} y_i}{n(\sum_{i=1}^{n} x_i^2) - (\sum_{i=1}^{n} x_i)^2} \tag{16}$$

where n is the number of data points.

VERTICAL SEISMIC PROFILE (VSP) DATA

In order to asses the effects of absorption on a given pulse and establish an empirical relation between the Lipschitz exponent α and the loss factor Q, a synthetic zero-offset VSP model for a single layer with varying velocity, depth and Q values is constructed. Applying the continuous wavelet transform to the given impulse response and subsequently estimating the corresponding modulus maxima values permits us to use the methods developed in the previous two chapters to estimate the corresponding Lipschitz values. The evolution of the Lipschitz values with depth is then to provide the necessary mathematical mapping relation between Q and α.

SYNTHETIC VSP MODELLING

For the initial VSP model, the wave velocity is set to a fixed value of $v = 2500m/s$, whereas the receiver depth and Q vary from $300m$ to $1600m$ and 10 to 200 respectively. The wavelet scale ranges from $j = 1$ to $j = 6$ with the sample rate and sample number set to $4ms$ and 512 respectively. As one would expect with decreasing Q, the pulse starts to lose amplitude and broaden in width. Hence, the expected Lipschitz value should shift from -1 to values closer to 0. In order to estimate the Lipschitz values, we need to minimise the following multivariable objective function

$$\phi(A, s, \sigma) = \sum_{i,j=1}^{n} [\log_2 |a_i| - \log_2 |A| - j + \frac{\alpha - 1}{2} \log_2(\sigma^2 + 2^{2j})]^2. \tag{17}$$

Figure 2 illustrates the maxima modulus values against wavelet scale corresponding to the direct arrivals at receiver locations $z = 270m$, $z = 630m$, $z = 1230m$ and $z = 1470m$ where $Q = 50$ and $v = 2500m/s$. Taking into consideration the fact that non-linearity in equation 17 stems from σ, the least squares minimisation method not only captures the non-linear segment given in figure 2, but provides an overall accurate fit to the data ($\log_2 |a_i|$ vs j). The total error between the data and least squares fit in figure 2 (a) to (d) is 0.0034, 0.0206, 0.0177 and 0.0438 respectively.

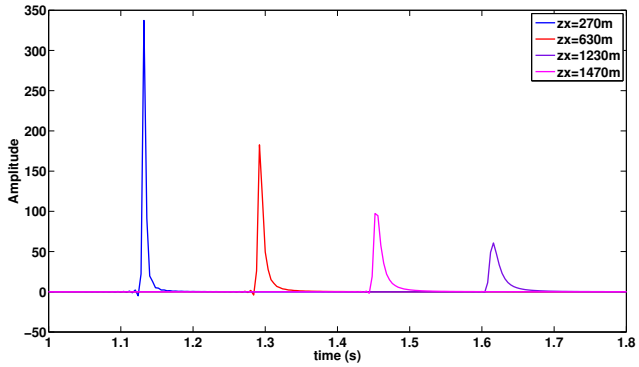

FIG. 1. Direct arrivals corresponding to receivers located at $z = 270m$, $z = 630m$, $z = 1230m$ and $z = 1470m$ respectively with $Q = 20$.

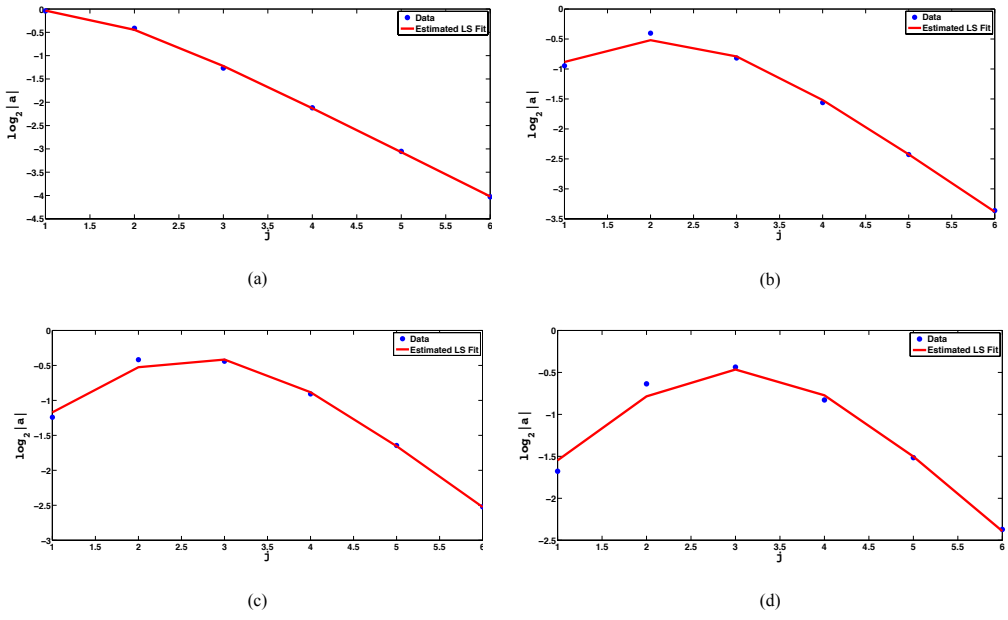

FIG. 2. $\log_2 |a_i|$ vs j for direct arrival at (a) $z = 270m$ (b) $z = 630m$ (c) $z = 1230m$ (d) $z = 1470m$.

THE RELATIONSHIP BETWEEN MHZ MODEL PARAMETERS AND *Q*

Plotting α against Q, could provide greater insight into the possible relation between the Lipschitz exponent and absorption. As illustrated in Figure 3 (a) it is clearly evident that for the α and Q, a trivial function or mathematical description providing a mapping between α and Q may not exist.

The relationship between Lipschitz regularity α and *Q*

Based on curve fitting method and certain degree of trial and error, in order to establish a mapping between α and Q one might consider the following function

$$\alpha = a_1 Q^m \ln Q + a_2 Q^m + a_3. \tag{18}$$

The solution to a_1, a_2 and a_3 is given by

$$A = (M^T M)^{-1} M^T Y \tag{19}$$

where

$$A = \begin{bmatrix} a_1 \\ a_2 \\ a_3 \end{bmatrix}, Y = \begin{bmatrix} \alpha_1 \\ \alpha_2 \\ \vdots \\ \alpha_n \end{bmatrix} \tag{20}$$

and

$$M = \begin{bmatrix} Q_1^m \ln Q_1 & Q_1^m & 1 \\ Q_2^m \ln Q_2 & Q_2^m & 1 \\ \vdots & \vdots & \vdots \\ Q_n^m \ln Q_n & Q_n^m & 1 \end{bmatrix}. \tag{21}$$

Hence, based on equation 18 one obtains the following relation

$$\alpha = 22.3210 Q^{-1.6} \ln Q - 63.2414 Q^{-1.6} - 1.0011. \tag{22}$$

The optimum value for *m* is obtained through trial and error. Figure 3 (b) illustrates the estimated fit to the data with a total error of $1.4472e-05$. However, one should be aware of the limitations associated with equation 18. As travel-time increases with increasing receiver depth, hence increasing absorption, the curvature or "kink" observed in Figure 3 seemingly flattens and shifts towards increasing *Q* values. Thus, one would need to exclude lower *Q* values in order to apply equation 18. Plotting α against *Q* for $z = 630m$ and $z = 1230m$ would require exclusion of *Q* values lower than 50 and 100 respectively (illustrated in Figures 4 and 5). Minimising and obtaining the solution to equation 18 yields the following

$$\alpha = 112.7576 Q^{-1.6} \ln Q - 423.1553 Q^{-1.6} - 1.0096 \tag{23}$$

and

$$\alpha = 291.5000 Q^{-1.6} \ln Q - 1293.700 Q^{-1.6} - 1.0000 \tag{24}$$

for $z = 630m$ and $z = 1230m$ respectively. The total error between data and estimated fit for $z = 630m$ is equal to $5.6745e-06$ and equal to $1.4286e-06$ for $z = 1230m$.

In contrast to Figure 3 (a), with increasing absorption due to increasing receiver depth, equation 18 fails to capture or estimate the data (α *vs* *Q*) in its entirety. For $z = 630m$ and $z = 1230m$, equation 18, only captures or provides an estimate to a portion of the data, as evident in Figures 4 and 5. Hence, equation 18 fails to provide a robust mathematical description between α and math Q for all possible model scenarios. Furthermore, one can not easily invert equation 18 in order to estimate *Q* values from α, thus limiting the probable application(s) associated with absorption and the Lipschitz exponent α.

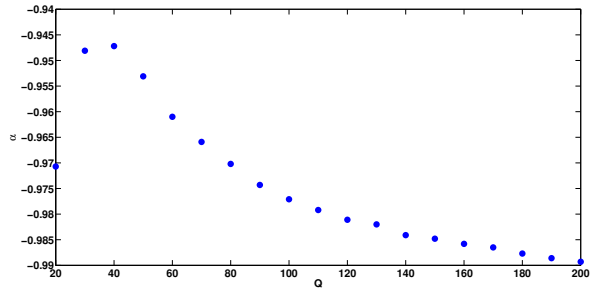

(a)

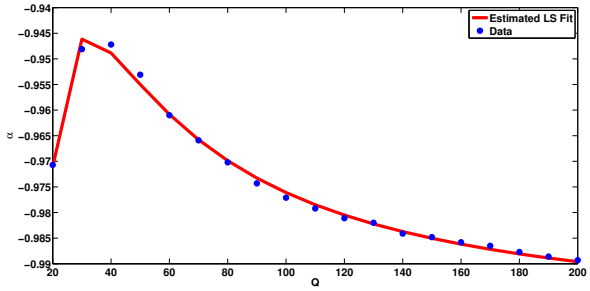

(b)

FIG. 3. (a) Plot of α *vs Q* for $z = 270m$ (b) Estimated Fit.

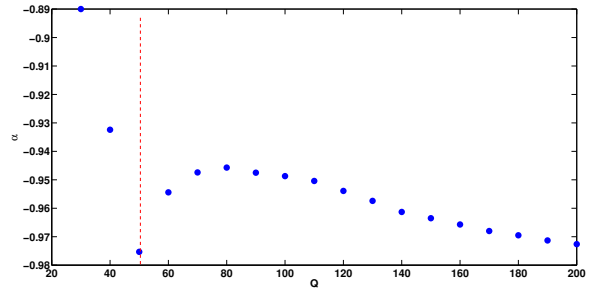

(a)

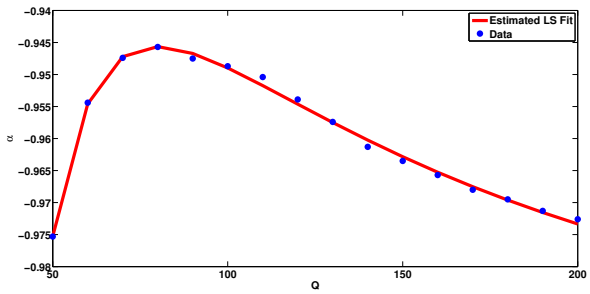

(b)

FIG. 4. (a) Plot of α *vs Q* for $z = 630m$ (b) Estimated Fit.

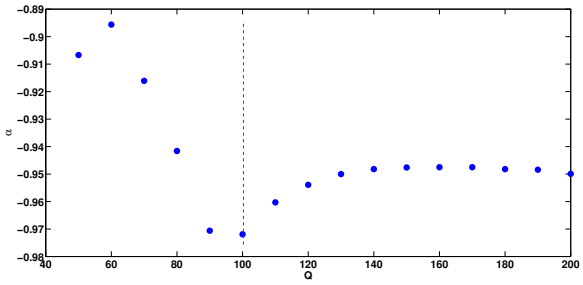

(a)

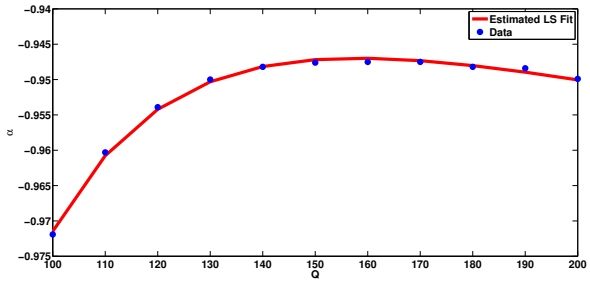

(b)

FIG. 5. (a) Plot of α *vs Q* for $z = 1230m$ (b) Estimated Fit.

The relationship between smoothness σ and Q

Given the limitations associated with the mathematical function mapping α to Q, one might consider the possible relation between the third parameter σ and Q. Contrary to α, plotting σ against Q values given in Table **??** reveals a relatively trivial power law type relation between the two variables. As illustrated in Figure 6, one could easily estimate a fit to the given data by the following relation

$$\sigma = b_1 Q^{b_2}. \tag{25}$$

For exponentially related data, one must linearise the problem and subsequently minimise using least squares method. Linearising equation 25 yields the following expression

$$\ln \sigma = \ln b_1 + b_2 \ln Q. \tag{26}$$

Hence, by minimising one obtains the following solutions

$$b_1 = \exp\left(\frac{\sum_{i=1}^{n} (\ln Q_i)^2 \sum_{i=1}^{n} \ln \sigma_i - \sum_{i=1}^{n} \ln Q_i \ln \sigma_i \sum_{i=1}^{n} \ln Q_i}{n(\sum_{i=1}^{n} (\ln Q_i)^2) - (\sum_{i=1}^{n} \ln Q_i)^2} \right) \tag{27}$$

and

$$b_2 = \frac{n\sum_{i=1}^{n} \ln Q_i \ln \sigma_i - \sum_{i=1}^{n} \ln Q_i \sum_{i=1}^{n} \ln \sigma_i}{n(\sum_{i=1}^{n} (\ln Q_i)^2) - (\sum_{i=1}^{n} \ln Q_i)^2}. \tag{28}$$

Plotting σ against logarithm of Q (figure 6 (b)), one could re-write equation 25 as

$$\sigma = b_1' \ln Q^{b_2'} \tag{29}$$

Subsequently minimising yields the following solution

$$b_1' = \exp\left(\frac{\sum_{i=1}^{n}(\ln(\ln Q_i))^2\sum_{i=1}^{n}\ln\sigma_i - \sum_{i=1}^{n}\ln(\ln Q_i)\ln\sigma_i\sum_{i=1}^{n}\ln(\ln Q_i)}{n(\sum_{i=1}^{n}(\ln(\ln Q_i))^2) - (\sum_{i=1}^{n}\ln(\ln Q_i))^2}\right) \tag{30}$$

and

$$b_2' = \frac{n\sum_{i=1}^{n}\ln(\ln Q_i)\ln\sigma_i - \sum_{i=1}^{n}\ln(\ln Q_i)\sum_{i=1}^{n}\ln\sigma_i}{n(\sum_{i=1}^{n}(\ln(\ln Q_i))^2) - (\sum_{i=1}^{n}\ln(\ln Q_i))^2}. \tag{31}$$

Additionally, one could improve the fit or estimation by applying additional weight on estimation points with lower error values relative to data points. Referred to as the weighted least squares method, an estimation to data is obtained based on the following mathematical expression

$$\min\sum_{i=1}^{n}\frac{[\ln\sigma_i - (\ln b_1 + b_2\ln Q_i)]^2}{(\sigma_i')^2} \tag{32}$$

where σ_i' is the standard deviation of the ith observation. Due to the limiting fact that our data consists of a single observation, the error between the least squares fit (without weights) and data points has been assigned as wights in the wighted least squares estimation.

Figure 6 illustrates the expected trend, such that increasing absorption broadens a given pulse, hence resulting in increasing σ values. Compared to the least squares approximation, the weighted least squares method slightly overestimates the given data. Additionally, plotting σ against $\ln Q$ and subsequently minimising yields the most accurate fit with a total error of 0.1825. The mathematical relation mapping σ and Q, for a receiver located at $z = 270m$, is given by

$$\sigma = 29.1085Q^{-0.7015} \tag{33}$$

and

$$\sigma = 21.4660Q^{-0.6390} \tag{34}$$

for least squares and weighed least squares respectively. Additionally, the relation between σ and $\ln Q$ for $z = 270m$ is given by

$$\sigma = 101.0296\ln Q^{-2.9492}. \tag{35}$$

Clearly, the addition of the third σ provides new insight and possibly a new avenue into the relation between the effects of absorption and applications of continuous wavelet transform. Contrary to the Lipschitz exponent, one obtains a relatively trivial mathematical function relating σ to the loss factor .

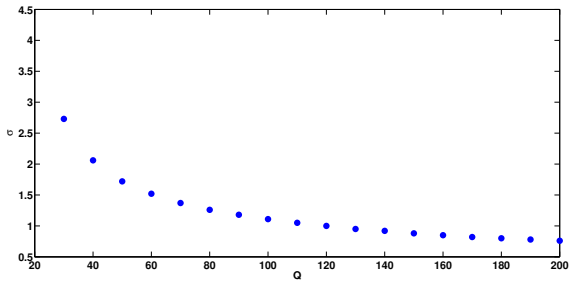

(a)

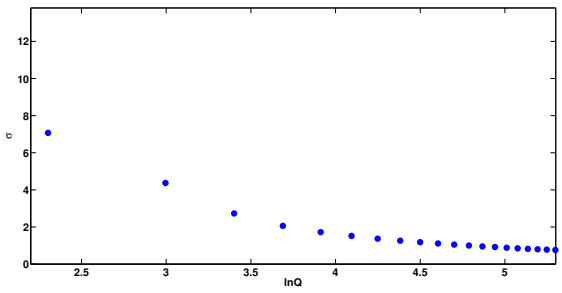

(b)

FIG. 6. Plot of (a) σ *vs* Q (b) σ *vs* $\ln Q$ for $z = 270m$.

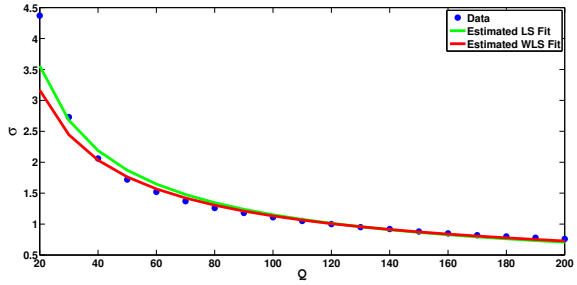

(a)

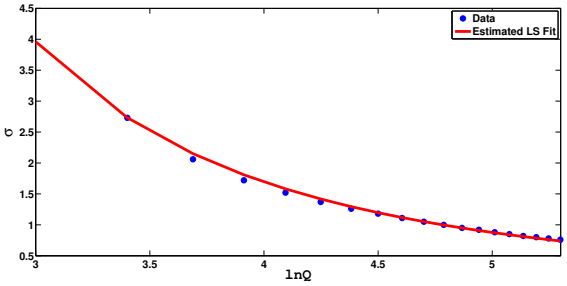

(b)

FIG. 7. (a) Plot of σ *vs* $Q\sigma$ *vs* $\ln Q$ (a) σ *vs* $\ln Q$ for $z = 270m$.

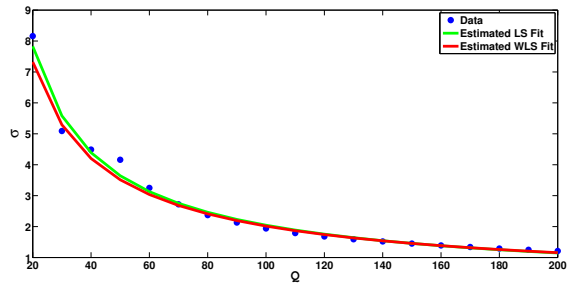

(a)

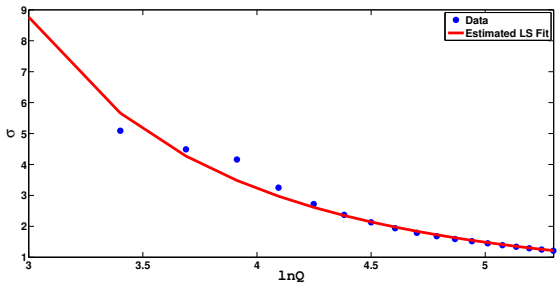

(b)

FIG. 8. Plot of (a) σ *vs* Q (b) σ *vs* $\ln Q$ for $z = 630m$.

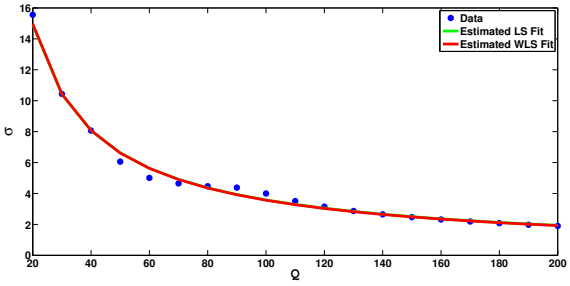

(a)

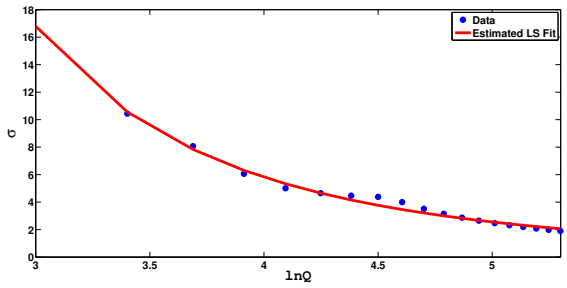

(b)

FIG. 9. Plot of (a) σ *vs* Q (b) σ *vs* $\ln Q$ for $z = 1230m$.

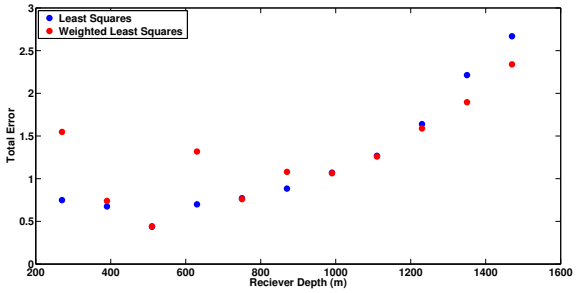

FIG. 10. Comparison of total errors associated with least squares and weighted least squares approximation.

Q estimation from MH model parameters

In contrast to the Lipschitz exponent (α), one could easily invert equations 25 and 29 in order to find a solution for Q. Hence, inverting, yields the following solutions

$$Q = \left(\frac{\sigma}{b_1}\right)^{\frac{1}{b_2}} \tag{36}$$

and

$$Q = \exp\left[\left(\frac{\sigma}{b_1'}\right)^{\frac{1}{b_2'}}\right]. \tag{37}$$

Using the σ values corresponding to $z = 270m$, the estimated Q values obtained from equation 36 provides a slightly more accurate estimate to true Q values with lower absolute error values. However, as illustrated in Figure fig:33 (a) and (b), with increasing absorption, equation 37 generally tends to approximate the true Q with higher degree of precision, thus lower absolute error values.

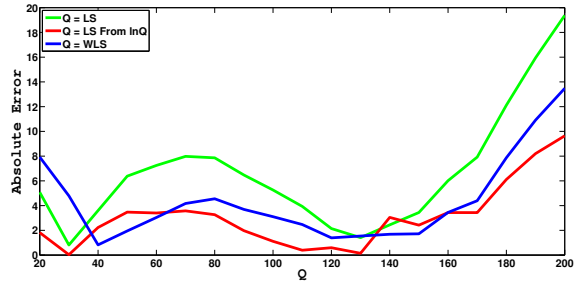

FIG. 11. Comparison of absolute errors for $z = 270m$.

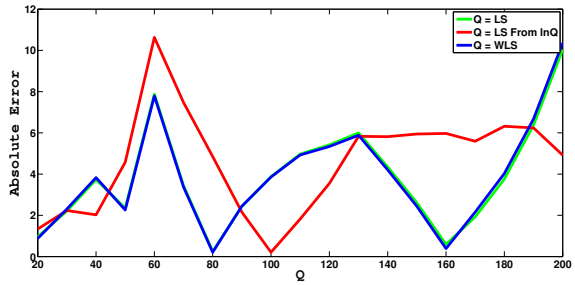

(a)

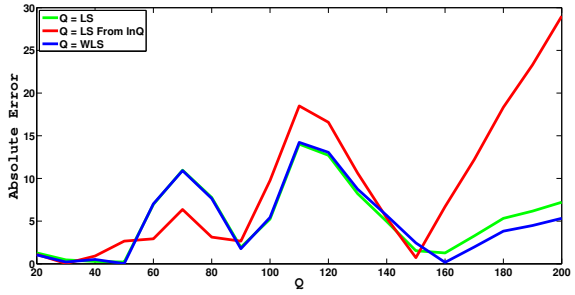

(b)

FIG. 12. Comparison of absolute errors associated with least squares, weighted least squares and $\sigma -> \ln Q$ approximation for (a) $z = 750m$ (b) $z = 1470m$.

APPLICATION TO THE ROSS LAKE VSP FIELD DATA SET

The validity, stability and ultimately viability of a mathematical model requires departure from a controlled setting, i.e. synthetic modelling, where inputs parameters are known, to an unknown, uncertain environment comprised of field data. The Ross Lake 3D VSP data, not only provides an opportunity to test, examine and analyse the behaviour of modulus maxima on field data, but also an opportunity to study the empirical relation between α, σ and Q obtained from synthetic modelling. In June 2003, the Ross Lake heavy oil field (located in south western Saskatchewan) was subject to a multi-offset VSP survey conducted by the CREWES project in conjunction with Husky Energy Inc. and Schlumberger Canada in order to study the relationship between rock properties and attenuation, AVO effect of the reservoir and improve the characterisation of the Cretaceous channel (Zhang, 2010).

The multi-offset VSP survey conducted by CREWES, Huskey Energy Inc. and Schlumberger Canada on June 2003, provided a detailed mapping of the Cantuar channel resevoir and further enhanced the interpretation of the 3C-3D seismic survey acquired in 2002 (Zhang, 2010). All conducted surveys, utilised downhole five-level, three-component VSP tools with vertical and horizontal vibrator sources used for zero-offset VSP survey and vertical vibrator sources used for both far-offset and walkaway VSP surveys (Zhang, 2010). For the zero-offset VSP survey, the horizontal component recorded reflected, transmitted and direct S-waves, whereas the vertical component mainly recoded the incoming P-waves. Hence, the horizontal and vertical components were used for processing SS and PP waves respectively (Zhang, 2010).

FIG. 13. Ross Lake heavy oil field, (Zhang, 2010).

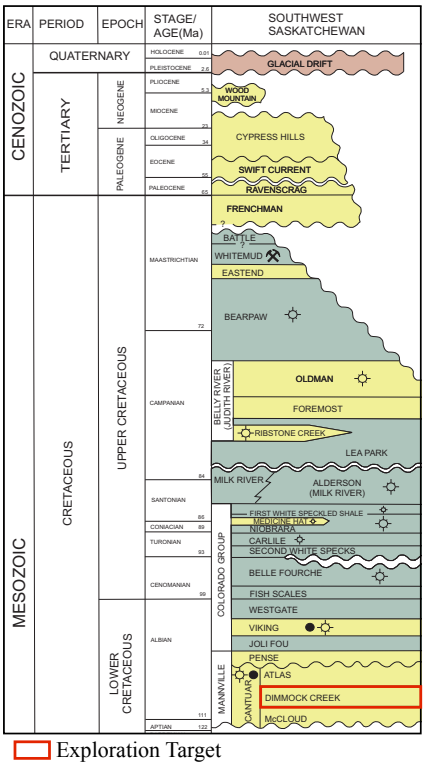

FIG. 14. Regional stratigraphic chart in southwest Saskatchewan (Saskatchewan Industry and Resources, 2006).

Survey Type	Zero-offset VSP	Far-offset VSP
Offset	$53.67m$	$399.12m$
Source Elevation	$856.10m$	$867.70m$
Source Azimuth	16.30^o	337.20^o
Source Type	Litton 315 P-vibe: Sweep$= 8 - 180$ Hz, IVI S-MINI vibe(inline): Sweep$= 5 - 100$ Hz; $12s$ linear sweep	Litton 315 P-vibe: Sweep$= 8 - 180$ Hz
Top Level	$197.50m$	$197.50m$
Bottom Level	$1165m$	$1165m$
Receiver Spacing	$7.50m$	$7.50m$
Reference Datum	KB$= 871.60m$	

Table 1. Aquistion parameters for Ross Lake VSP survey (Zhang, 2008).

Q in the Ross Lake VSP data

Whether the established empirical relation between σ and Q, obtained from synthetic data is applicable to field data, hinges on the behaviour modulus maxima values applied field data. Figure 15 (a), represents the downgoing P-wave corresponding to the far-offset VSP survey. The offset value for this particular VSP survey is equal to $x = 399.12m$, with a total of 119 receivers spaced $7.5m$ apart where the first receiver is located at a depth of $z = 197.50m$. Additionally, the corresponding VSP survey has a total number of 3001 samples with a sampling rate of $1ms$. Figure 15 (b), represents the trace of direct P-wave arrivals corresponding to the 5th, 20th, 50th and 100th receiver. It is clearly evident that the progressive amplitude decay implies a degree of absorption. Hence, based on theoretical properties and synthetic results, applying the continuous wavelet transform to the VSP data, calculating the corresponding modulus maxima values and plotting the logarithm against wavelet scale should exhibit a certain degree of sensitivity to absorption within the data. Minimising the following equation,

$$\log_2 |a_i| - j = \log_2 |A| - \frac{\alpha - 1}{2} \log_2(\sigma^2 + 2^{2j}) \tag{38}$$

yields an estimate to α, σ and subsequently provides an approximation to the data.

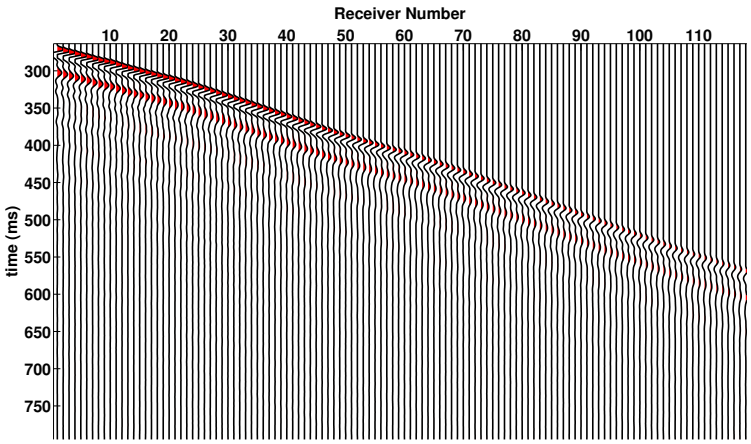

FIG. 15. Downgoing P-wave corresponding to the far-offset VSP survey.

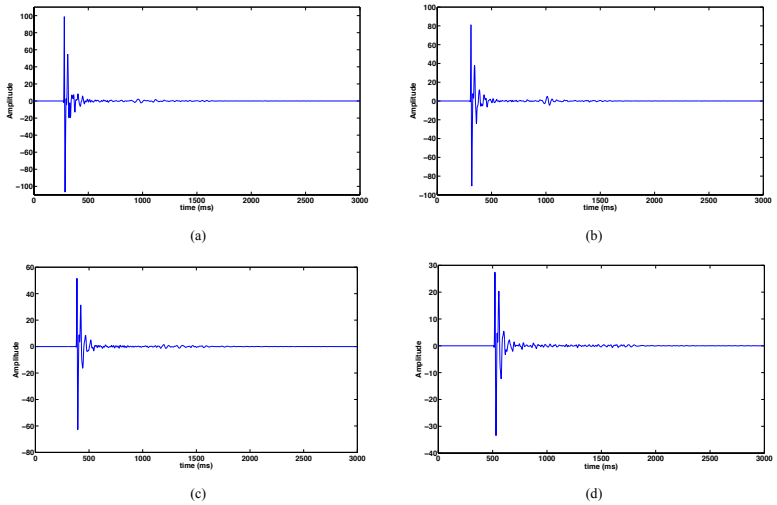

FIG. 16. Trace of direct P-wave arrival corresponding to the (a) 5th, (b) 20th, (c) 50th and (d) 100th receiver.

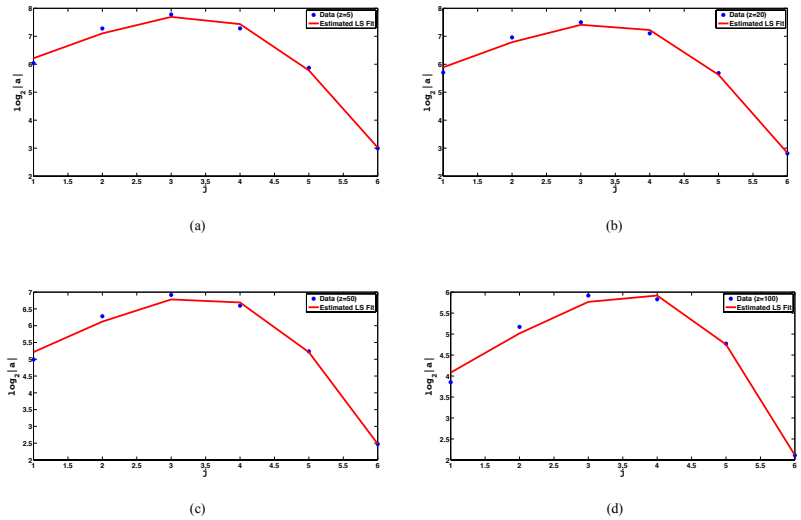

FIG. 17. $\log_2 |a_i|$ vs scale for P-wave corresponding to the (a) 5th, (b) 20th, (c) 50th and (d) 100th receiver respectively.

Figure 17, represents the logarithm of modulus maxima values against scale for the P-wave arrival corresponding to the 5th, 20th, 50th and 100th receiver. With increasing absorption, hence decay in amplitude, one could observe a gradual, progressive shift in curvature with increasing scale (from Figure 17 (a) to (d)). For field data, such gradual shift in curvature within data is encouraging, since it is via curvature that the model captures the effects of absorption, hence, it confirms and validates the sensitivity of the model to absorption. The total error between the least squares approximation and data corresponding to Figure 17 (a) to (d) is 0.1023, 0.0909, 0.1013 and 0.1077 respectively. Thus, the relatively small error between the least squares fit to data yields an opportunity to estimate Q based on the existing mathematical relation between σ and the loss factor obtained from synthetic modelling. Figure 17, illustrates increasing σ values with increasing receiver depth, hence an increase in absorption with increasing depth. The sudden "bump"

or increase in σ values roughly corresponding to the 50th to 70th receiver indicates a sudden increase in absorption. This could imply decrease in velocity, thus resulting in greater degree of absorption.

Estimating Ross Lake MHZ parameters and Q

Figure 18 represents the measured σ values corresponding to the respective receiver. In order to estimate the corresponding Q values, we need to measure the local σ values. With the exception of the first σ value, the remaining values represent the cumulative Q effects from previous layers. Mathematically, the cumulative effect could be represented as follows,

$$\sigma_n \propto \sum_{n=1}^{m} Q_n \tag{39}$$

where n represents the corresponding layer. In order to exclude the cumulative Q effects from previous layers and measure the local σ value(s), we deduct the two successive σ values from each other. For example, in order to estimate the local σ value corresponding to the second receiver, we deduct the first value from the second σ value as follows,

$$\sigma_{local\_2} = \sigma_2 - \sigma_1 \Longrightarrow \sigma_{local\_2} \propto Q_2 + Q_1 - Q_1 = Q_2. \tag{40}$$

Repeating the process provides an estimate to the local σ values corresponding to each receiver. Figure 19, represents the estimated local σ values corresponding to each receiver. Clearly, the highest value ($\sigma_{local\_1} = 18.2800$) indicates high degree of absorption within the first layer (from source to the first receiver). However, based on the Figure 19 the estimated local σ values (excluding the first value) reveal negligible yet gradual absorption, with the maximum local σ value equal to 0.8600. As a result, the medium has been subdivided into six intervals or layers, hence measuring the average Q value corresponding to each layer. Table 2 represents the σ values corresponding to each layer. It should be noted that the σ corresponding to the second layer is calculated by deducting the the local σ value corresponding to the first receiver from the σ corresponding to the 34th receiver (located at $z = 450m$). Hence the estimated local σ value corresponds to the average Q values from $z = 200m$ to $z = 450m$. The rest of the σ values (corresponding to the remaining layers) are estimated in similar fashion.

Depth(m)	Local σ value
$7 - 200$	18.2800
$200 - 450$	1.3000
$450 - 600$	2.4300
$600 - 800$	1.4800
$800 - 1000$	2.3600
$1000 - 1165$	1.2400

Table 2. Corresponding depth and local σ values.

Applying the minimum and mid-range values given in Table 3 to equations 25 and 29, yields unrealistic Q values corresponding to the first layer, with minimum Q values ranging from roughly 1.2859 to just under 15. However, the remaining Q values range from high twenties to just under 270, a relatively acceptable range. Additionally, applying

the maximum obtained values yields Q estimates ranging from roughly 20 to Q values slightly over 600. Figure 20, represented the estimated Q values using equations 36 and 37. For the minimum and mid-range values equation 36 and 36 provide Q values in relative close proximity. However, using the maximum values given in Table 3, equation 37 seems to overestimate the measured Q values.

	Minimum Value	Mid-level Value	Maximum Value
b_1	29.1085	149.8336	259.5581
b_2	-0.7015	-0.8765	-0.8787
b_{1w}	21.4660	138.9541	261.0325
$b2_w$	-0.6390	-0.8617	-0.8807
$b_1^{'}$	101.0296	662.0009	1176.3000
$b_2^{'}$	-2.9492	-3.6388	-3.6624

Table 3. Maximum, medium-range and minimum coefficient values from synthetic modelling were b_1, b_2 is obtained from least squares method and b_{1w}, b_{2w} is obtained from weighted least squares method.

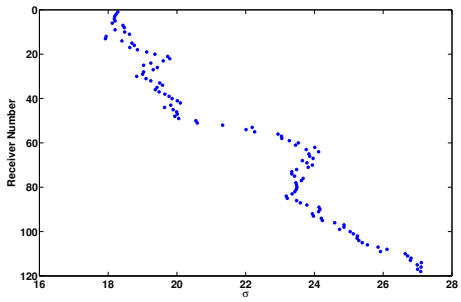

FIG. 18. Plot of estimated σ values against receiver number.

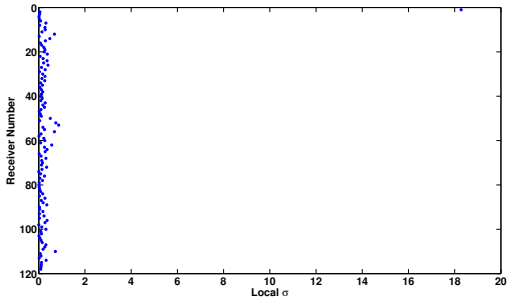

FIG. 19. Plot of estimated local σ values against receiver number.

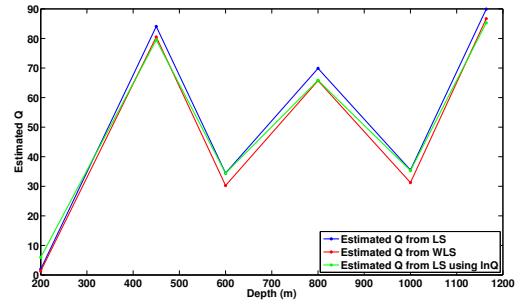

(a)

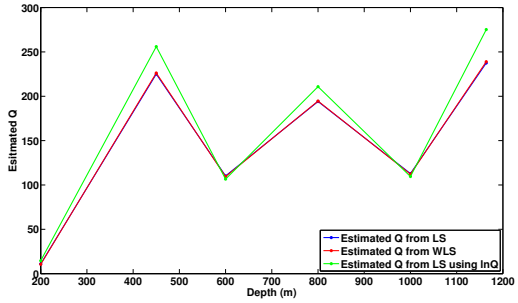

(b)

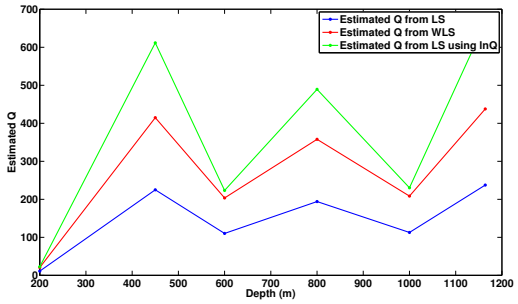

(c)

FIG. 20. Estimated *Q* values using equation 36 and 37 with (a) Minimum obtained values given in Table 3 (b) Mid-level obtained values given in Table 3 (c) Maximum obtained values given in Table 3.

From an interval of $z = 200m$ to $z = 1000m$ the Q_p values estimated by Xu and Stewart (2004) generally reveals a downward trend in Q_p values with a maximum value of $Q_p = 197$ and minimum value of $Q_p = 28$. Hence, for the most part absorption seems to be increasing. For the deepest interval, $z = 1000m$ to $z = 1165m$, absorption seems to decrease with Q_p value of 136. The general trend for absorption (from $z = 450m - 1165m$) seems to be captured by the estimated σ and Q values, with the minimum and mid-level values provided in Table 3 yielding relatively accurate Q values to the estimated values using the spectral ration method.

CONCLUSION

The continuous wavelet transform and the associated Lipschitz regularity provide a potentially efficient and powerful tool for analysing singularities in a signal. For a single event, a linear model enables us to estimate the Lipschitz exponent and characterise the singularity with relative ease.

An accurate estimation of signal regularity and smoothness for varying Q values (corresponding to VSP model) provides an opportunity to mathematically map Q to α and σ. Plotting the α against a range Q values corresponding to a single receiver within the VSP Model, does not provide a trivial mathematical relation. Furthermore, the obtained mathematical function (mapping Q and α) is limited to a certain range of Q values or absorption levels. However, plotting the smoothness parameter σ against Q does provide a relatively trivial, power law type relation between the two parameters. Additionally, inverting the obtained relation, does provide accurate Q values in comparison to the original values.

Applying the obtained mathematical relation between σ and Q (from synthetic VSP modelling) to the Ross Lake field data provides mixed results. Compared to the spectral ratio method, the Q values estimated from the obtained power law relation falls short. However, a positive and encouraging sign relates to the fact that the re-arranged non-linear MHZ model does capture the effects of absorption on a seismic signal. Hence, a theoretical and practical framework exists, such that additional research could potentially lead to a robust mathematical relation between smoothness and Q.

REFERENCES

Burden, R. L., and Douglas, F. J., 2005, Numerical Analysis: Thomson Books/Cole, 8 edn.

Gao, R. E., and Yan, R., 2011, Wavelets: Theory and Applications for Manufacturing: Springer.

Hermann, F. J., 1997, A scaling medium representation, a discussion on well-logs, fractals and waves: Ph.D. thesis, Technische Universiteit Delft.

Innanen, K. A., 2003, Local signal regularity and lipschitz exponents as a means to estimate Q: Seismic Exploration, , No. 12, 53–74.

Kjartansson, E., 1979, Attenuation of seismic waves in rocks and applications in energy exploration: Ph.D. thesis, Stanford University.

Mallat, S., and Hwang, L., 1992, Singularity detection and processing with wavelets: IEEE Transactions on Information Theory, **38**, No. 2.

Mallat, S., and Zhong, S., 1992, Characterisation of signals from multiscale edges: IEEE Transactions on Pattern Analysis and Machine Intelligence, **14**, No. 7.

Qian, S., 2002, Introduction to Time-Frequency and Wavelet Transforms: Prentice Hall PTR.

Zhang, C., 2008, Seismic absorption estimation and compensation: Ph.D. thesis, University of British Columbia.

Zhang, Z., 2010, Assessing attenuation, fractures, and anisotropy using logs, vertical seismic profile, and three-component seismic data: heavy oilfield and potash mining examples: Ph.D. thesis, University of Calgary.